Surface polaritons and extinction properties of a left-handed material cylinder

2004 J. Phys.: Condens. Matter 16 5991

(http://iopscience.iop.org/0953-8984/16/34/001)

INSTITUTE OF PHYSICS PUBLISHING JOURNAL OF PHYSICS: CONDENSED MATTER

J. Phys.: Condens. Matter **16** (2004) 5991–5998 PII: S0953-8984(04)81082-8

Surface polaritons and extinction properties of a left-handed material cylinder

R Ruppin[1]

Nanophotonics and Metrology Laboratory, EPFL, 1015 Lausanne, Switzerland

Received 21 May 2004
Published 13 August 2004
Online at stacks.iop.org/JPhysCM/16/5991
doi:10.1088/0953-8984/16/34/001

Abstract

The dispersion curves of the surface polaritons of a cylinder which is made of a material with dispersive permittivity and permeability, and which is left-handed over a frequency band, are calculated. It is found that there exist three surface mode bands. With increasing wavevector the three bands converge to three limiting frequencies, which are equal to the three corresponding frequencies obtained for the slab geometry. The extinction properties of the cylinder are derived, and the dependence of the extinction spectrum on the cylinder radius is investigated.

1. Introduction

The electromagnetic properties of a material, in which both the permittivity and the permeability assume negative values, have been analysed by Veselago [1]. Recently, such left-handed materials (LHM) have been produced by combining arrays of metallic wires and split-ring resonators [2]. The predicted negative refraction properties of these materials [1] have been confirmed experimentally [3, 4]. Another prediction of Veselago was that a LHM slab with a refractive index $n = -1$, would behave as a lens. Furthermore, Pendry [5] has shown that such a slab acts as a perfect lens whose resolution is not limited by the classical diffraction limit. This is because the slab acts as a lens not only for propagating waves, but also for the evanescent near field radiation, due to the excitation of surface polariton states [6]. The possibilities of spherical and cylindrical perfect lenses made of negative refractive index materials have also been discussed recently [7, 8].

Here we investigate the electromagnetic properties of a cylinder made of a LHM. We obtain the dispersion curves of the surface polariton modes, i.e. the modes which have evanescent behaviour both inside and outside the cylinder. We also calculate the extinction spectra of the LHM cylinder, when irradiated by a normally incident plane wave.

[1] On leave from: Soreq NRC, Yavne 81800, Israel.

2. Surface modes of left-handed material cylinder

We consider a cylinder of radius a, with relative permittivity $\varepsilon(\omega)$ and relative permeability $\mu(\omega)$. The relative permittivity and permeability of the medium surrounding the cylinder, μ_{m} and ε_{m}, are assumed to be frequency independent. Using cylindrical coordinates (r, θ, z), the dispersion equation for the eigenmodes having a $\exp(\mathrm{i}qz + \mathrm{i}n\theta)$ z and θ dependence is given by [9]

$$\left[\frac{\mu}{u}\frac{J_n'(u)}{J_n(u)} - \frac{\mu_{\mathrm{m}}}{v}\frac{H_n'(v)}{H_n(v)}\right]\left[\frac{k_i^2}{\mu u}\frac{J_n'(u)}{J_n(u)} - \frac{k_0^2}{\mu_{\mathrm{m}} v}\frac{H_n'(v)}{H_n(v)}\right] = n^2q^2\left(\frac{1}{v^2} - \frac{1}{u^2}\right)^2. \tag{1}$$

Here $k_i = k_0\sqrt{\varepsilon\mu}$, $k_{\mathrm{m}} = k_0\sqrt{\varepsilon_{\mathrm{m}}\mu_{\mathrm{m}}}$, where $k_0 = \omega\sqrt{\varepsilon_0\mu_0}$ is the free space wavenumber. J_n and H_n are Bessel and Hankel functions, respectively, with $u = \sqrt{k_i^2 - q^2}a$ and $v = \sqrt{k_{\mathrm{m}}^2 - q^2}a$.

The (q, ω) plane can be divided into a number of separate regions according to the behaviour of the electromagnetic fields inside and outside the cylinder. To demonstrate this classification, we choose the following forms of the permittivity and the permeability, typical to left-handed materials [10]

$$\varepsilon(\omega) = 1 - \frac{\omega_{\mathrm{p}}^2}{\omega^2} \tag{2}$$

$$\mu(\omega) = 1 - \frac{F\omega_0^2}{\omega^2 - \omega_0^2}. \tag{3}$$

In the numerical calculations the following values will be employed: plasma frequency, $\omega_{\mathrm{p}} = 10$ GHz, magnetic resonance frequency, $\omega_0 = 4$ GHz and $F = 1.25$. With this choice of parameters, the frequency range in which both $\varepsilon(\omega)$ and $\mu(\omega)$ are negative, so that the cylinder material is left-handed, extends from 4 to 6 GHz.

The radial behaviour of the fields outside the cylinder is oscillatory for $k_{\mathrm{m}}^2 > q^2$, and evanescent for $q^2 > k_{\mathrm{m}}^2$. Similarly, the radial behaviour of the fields inside the cylinder is oscillatory for $k_i^2 > q^2$ and evanescent for $q^2 > k_i^2$. This yields the six regions in the (q, ω) plane shown in figure 1. Regions R_1, R_2, R_3 constitute the radiative region, in which the external fields are oscillatory, whereas in regions S_1, S_2, S_3 the external fields decay, essentially exponentially, with distance from the cylinder. In regions R_1, R_3, S_1, S_3 the field dependence on r within the cylinder is non-oscillatory, while in R_2 and S_2 it is oscillatory. We will calculate the dispersion of the pure surface modes, i.e. the modes that are characterized by radially evanescent fields both inside and outside the cylinder, since these are of interest for potential applications of left-handed materials. From the classification shown above, we find that these modes are restricted to regions S_1 and S_3. We have calculated the dispersion of the $n = 0, 1, 2, 3$ surface modes, for a cylinder of radius a, given by $\omega_0 a/c = 0.5$, and the results are shown in figure 2. For each value of n there exist three surface modes, one in region S_1 (band (a)) and two in region S_3 (bands (b) and (c)). In each of the three surface mode series, the $n = 0$ mode is the lowest, and the frequency increases with n. We note the limiting values of the surface mode frequencies for large q. The lowest band, (a), in region S_1, converges to the frequency ω_0. The middle band, (b), in region S_3, converges to the frequency ω_1, given by $\mu(\omega_1) = -\mu_{\mathrm{m}}$. The highest band, (c), also in region S_3, converges to the frequency ω_2, given by $\varepsilon(\omega_2) = -\varepsilon_{\mathrm{m}}$. These limiting values coincide with the corresponding large q limits of the surface polariton frequencies at a plane interface between the two media [11]. This could be expected, since in the limit of extreme localization the frequencies of the cylinder surface modes become independent of the finite curvature of the surface.

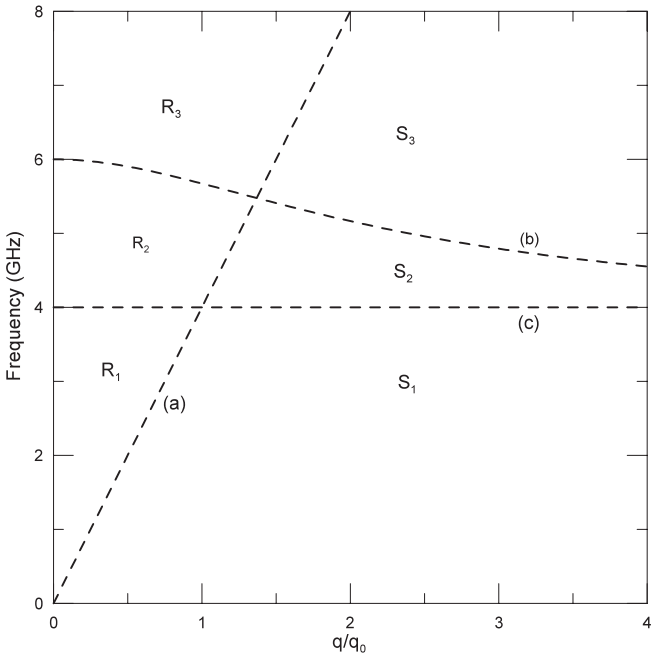

Figure 1. Regions in the (q, ω) plane, where q, the wavevector component parallel to the cylinder axis, is expressed in units of $q_0 = \omega/c$. The curves which define the boundaries between the regions are: (a) $q = \sqrt{\varepsilon_m \mu_m}\omega/c$; (b) $q = \sqrt{\varepsilon(\omega)\mu(\omega)}\omega/c$; (c) $\omega = \omega_0$.

Due to their evanescent behaviour outside the cylinder, the surface polaritons analysed in this section do not interact with an externally applied electromagnetic plane wave. Such a wave can only interact with polaritons in the radiative regions R_1, R_2 and R_3. This interaction will be discussed in the next section, where the electromagnetic scattering properties of the LHM cylinder are derived.

3. Scattering by a dielectric-magnetic cylinder

Since in the textbook solutions for the electromagnetic scattering properties of dielectric cylinders [12, 13] it is assumed that they are non-magnetic (i.e. their permeability is equal to the vacuum value μ_0) we outline here the solution for the magnetic case. We then describe how the fact that the cylinder material is LHM manifests itself in the extinction spectra.

We assume a normally incident plane wave, with the magnetic field polarization parallel to the cylinder axis (TE polarization). All the fields are expanded in terms of the cylindrical vector wavefunctions [14]

$$\vec{M}_n = \vec{\nabla} \times [\hat{a}_z Z_n(kr) \exp(\mathrm{i}n\theta)] \tag{4}$$

$$\vec{N}_n = (1/k)\vec{\nabla} \times \vec{M}_n. \tag{5}$$

Here $\hat{a}_z$ is a unit vector in the z direction, $Z_n(kr)$ represents a cylindrical Bessel or Hankel function, and is chosen as follows. Inside the cylinder $J_n(k_i r)$ is used and outside the cylinder $J_n(k_m r)$ and $H_n(k_m r)$ are used for the incident and scattered waves, respectively.

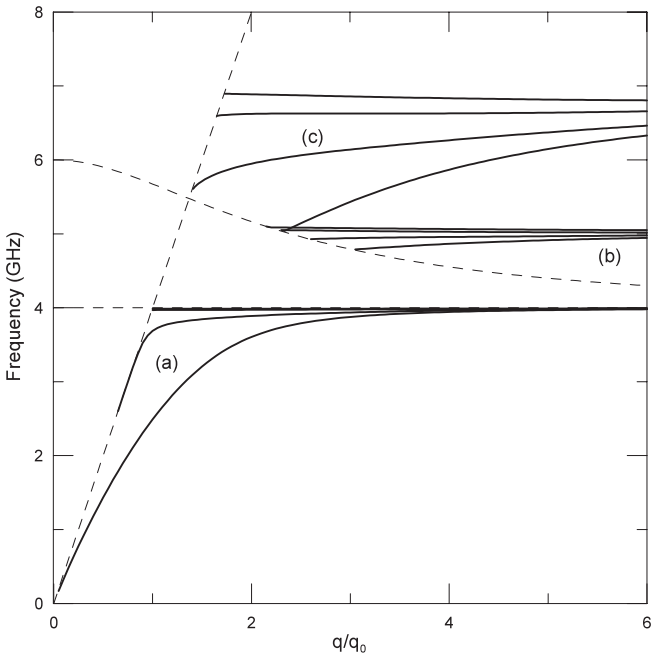

Figure 2. Dispersion curves of $n = 0, 1, 2, 3$ surface polaritons for a cylinder with radius a given by $\omega_0 a/c = 0.5$.

The fields of the incident wave are given by [12]

$$\vec{E}^{\mathrm{i}} = E_0 \exp(\mathrm{i}k_{\mathrm{m}}x)\,\widehat{a}_y = \mathrm{i}(E_0/k_{\mathrm{m}}) \sum_{n=-\infty}^{\infty} \mathrm{i}^n \vec{M}_n(k_{\mathrm{m}}r) \tag{6}$$

$$\vec{H}^{\mathrm{i}} = (1/\mathrm{i}\omega\mu_0\mu_{\mathrm{m}})\vec{\nabla} \times \vec{E}^{\mathrm{i}} = (E_0/\omega\mu_0\mu_{\mathrm{m}}) \sum_{n=-\infty}^{\infty} \mathrm{i}^n \vec{N}_n(k_{\mathrm{m}}r). \tag{7}$$

The transmitted fields inside the cylinder are expanded in the form

$$\vec{E}^{\mathrm{t}} = \mathrm{i}(E_0/k_i) \sum_{n=-\infty}^{\infty} \mathrm{i}^n d_n \vec{M}_n(k_i r) \tag{8}$$

$$\vec{H}^{\mathrm{t}} = (E_0/\omega\mu_0\mu) \sum_{n=-\infty}^{\infty} \mathrm{i}^n d_n \vec{N}_n(k_i r) \tag{9}$$

and the scattered fields expansion is

$$\vec{E}_{\mathrm{s}} = \mathrm{i}(E_0/k_0) \sum_{n=-\infty}^{\infty} \mathrm{i}^n a_n \vec{M}_n(k_{\mathrm{m}}r) \tag{10}$$

$$\vec{H}_{\mathrm{s}} = (E_0/\omega\mu_0\mu_{\mathrm{m}}) \sum_{n=-\infty}^{\infty} \mathrm{i}^n a_n \vec{N}_n(k_{\mathrm{m}}r). \tag{11}$$

The unknown expansion coefficients a_n and d_n are determined by the boundary conditions at the surface of the cylinder. Requiring the tangential components of the electric and magnetic fields to be continuous yields the equations

$$J_n'(k_{\mathrm{m}}a)/k_{\mathrm{m}} + a_n H_n'(k_{\mathrm{m}}a)/k_{\mathrm{m}} = d_n J_n'(k_i a)/k_i \tag{12}$$

$$J_n(k_{\mathrm{m}}a)/\mu_{\mathrm{m}} + a_n H_n(k_{\mathrm{m}}a)/\mu_{\mathrm{m}} = d_n J_n(k_i a)/\mu. \tag{13}$$

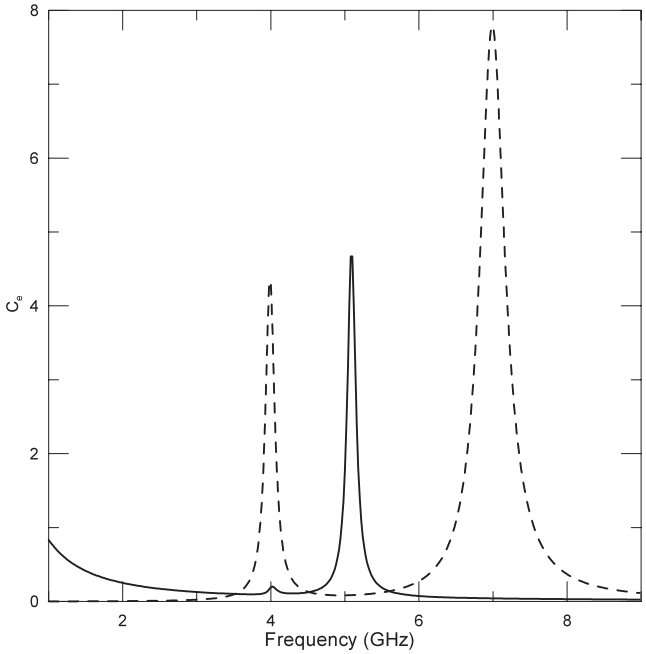

Figure 3. Extinction spectrum of a LHM cylinder of radius 0.1 cm. Full curve—TM polarization; broken curve—TE polarization.

From these equations it is found that the scattered field coefficients are given by

$$a_n = -\frac{\eta_{\rm m} J_n'(k_{\rm m}a) J_n(k_i a) - \eta J_n(k_{\rm m}a) J_n'(k_i a)}{\eta_{\rm m} H_n'(k_{\rm m}a) J_n(k_i a) - \eta H_n(k_{\rm m}a) J_n'(k_i a)} \tag{14}$$

where $\eta_{\rm m} = \sqrt{\mu_{\rm m}/\varepsilon_{\rm m}}$ and $\eta = \sqrt{\mu/\varepsilon}$.

When both the surrounding medium and the cylinder material are non-magnetic (i.e. $\mu = \mu_{\rm m} = 1$) the coefficients a_n reduce to the well known expressions for dielectric cylinders [12, 13].

The case in which the electric field polarization is parallel to the cylinder axis (TM polarization) has been treated before [15], and the scattering coefficients have been shown to be given by

$$b_n = -\frac{\eta_{\rm m} J_n(k_{\rm m}a) J_n'(k_i a) - \eta J_n'(k_{\rm m}a) J_n(k_i a)}{\eta_{\rm m} H_n(k_{\rm m}a) J_n'(k_i a) - \eta H_n'(k_{\rm m}a) J_n(k_i a)}. \tag{15}$$

We note that the scattering coefficients given by equations (14) and (15) differ from those employed in a recent work on the scattering properties of a LHM cylinder [16].

The optical properties of the cylinder are expressed in terms of widths, which are defined as the cross-sections per unit length of the cylinder. These will be presented in a dimensionless form, in units of the geometric width $2a$. The extinction width of the cylinder is given by [12, 13]

$$C_{\rm e} = -(2/k_{\rm m}a) \sum_{n=-\infty}^{\infty} {\rm Re}\, a_n \tag{16}$$

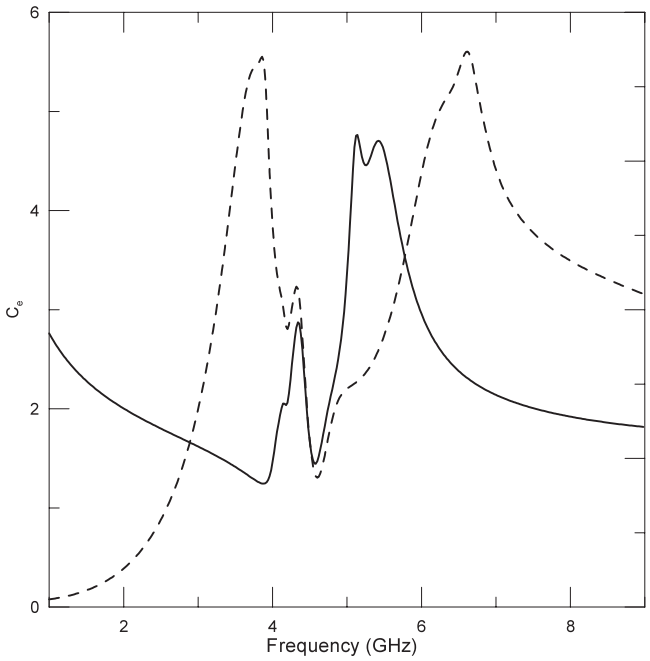

Figure 4. Extinction spectrum of a LHM cylinder of radius 1 cm. Full curve—TM polarization; broken curve—TE polarization.

for the TE polarization and by

$$C_{\mathrm{e}} = -(2/k_{\mathrm{m}}a)\sum_{n=-\infty}^{\infty} \mathrm{Re}\, b_n \tag{17}$$

for the TM polarization.

4. Numerical results and discussion

Using equations (16) and (17) we have calculated the extinction of LHM cylinders having a permittivity of the form (2) and a permeability of the form (3), but with a damping term $\gamma = 0.03$ added to both. The extinction spectrum of a very thin cylinder, of radius 0.1 cm, is shown in figure 3. In this small size limit, the electrostatic and magnetostatic fields are decoupled, the fields inside the cylinder are uniform, and the following simple interpretation of the extinction peaks applies. By considering the contribution of the depolarization field, it follows that the resonant frequencies, ω_i, of the electrostatic modes are given by

$$\varepsilon(\omega_i) = \varepsilon_{\mathrm{m}}\left(1 - \frac{4\pi}{N_i}\right) \tag{18}$$

where N_i is the depolarization factor for the given field direction. Similarly, the resonant frequencies of the magnetostatic modes are given by

$$\mu(\omega_i) = \mu_{\mathrm{m}}\left(1 - \frac{4\pi}{N_i}\right). \tag{19}$$

The depolarization factors of the cylinder are 2π for a field direction perpendicular to the cylinder, and zero for a field direction parallel to the cylinder. The corresponding magnetostatic

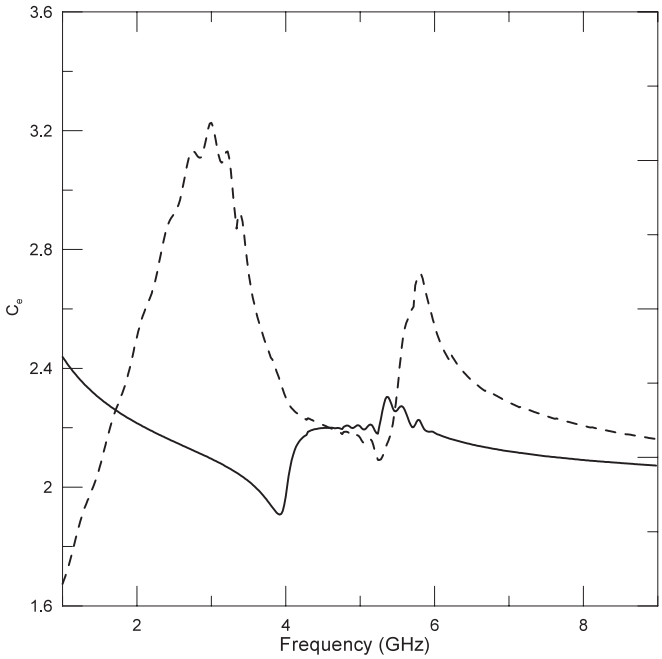

Figure 5. Extinction spectrum of a LHM cylinder of radius 10 cm. Full curve—TM polarization; broken curve—TE polarization.

mode frequencies are given by the resonance frequency, ω_0, of $\mu(\omega)$ when the magnetic field is parallel to the cylinder axis (lower peak, at 4 GHz, of the broken curve of figure 3), and by the frequency ω_1, given by $\mu(\omega_1) = -\mu_m$, when the magnetic field is perpendicular to the cylinder axis (peak at 5.1 GHz of the full curve). The electrostatic mode frequency is given by $\varepsilon(\omega_2) = -\varepsilon_m$ when the electric field is perpendicular to the cylinder axis (peak at 7 GHz of the broken curve). When the cylinder radius is increased to 1 cm the spectra shown in figure 4 are obtained. Each of the three narrow peaks of figure 3 evolves into a broader band consisting of a number of subsidiary peaks. For the parallel polarization (full curve of figure 4) a band of magnetic modes appears in the frequency region between 4 and 6 GHz in which the material is left-handed. For the perpendicular polarization (broken curve of figure 4), there appear electric surface modes above 6 GHz and below 4 GHz. The spectra obtained for an even larger radius of 10 cm are shown in figure 5. Only two prominent bands remain: the electric surface modes below 4 GHz and near 6 GHz. The spectrum tends to flatten out in the region just above the magnetic resonance frequency of 4 GHz. A similar phenomenon was found for large spheres [17], and it results from the fact that in this frequency region the medium is transparent (because the real part of both ε and μ are negative), so that highly localized surface modes cannot be sustained.

References

[1] Veselago V G 1968 *Sov. Phys.—Usp.* **10** 509
[2] Smith D R, Padilla W J, Vier D C, Nemat-Nasser S C and Schultz S 2000 *Phys. Rev. Lett.* **84** 4184
[3] Parazzoli C G, Greegor R B, Li K, Koltenbah B E C and Tanielian M 2003 *Phys. Rev. Lett.* **90** 107401
[4] Houck A A, Brock J B and Chuang I L 2003 *Phys. Rev. Lett.* **90** 137401
[5] Pendry J B 2000 *Phys. Rev. Lett.* **85** 3966

[6] Ruppin R 2001 *J. Phys.: Condens. Matter* **13** 1811
[7] Pendry J B and Ramakrishna S A 2003 *J. Phys.: Condens. Matter* **15** 6345
[8] Pendry J B 2003 *Opt. Express* **11** 755
[9] Stratton J A 1941 *Electromagnetic Theory* (New York: McGraw-Hill)
[10] Smith D R and Kroll N 2000 *Phys. Rev. Lett.* **85** 2933
[11] Ruppin R 2000 *Phys. Lett.* A **277** 61
[12] van de Hulst H C 1957 *Light Scattering by Small Particles* (New York: Wiley)
[13] Kerker M 1969 *The Scattering of Light and Other Electromagnetic Radiation* (New York: Academic)
[14] Morse P M and Feshbach H 1953 *Methods of Theoretical Physics* (New York: McGraw-Hill)
[15] Ruppin R 2003 *Microw. Opt. Technol. Lett.* **36** 150
[16] Kuzmiak V and Maradudin A A 2002 *Phys. Rev.* B **66** 045116
[17] Ruppin R 2000 *Solid State Commun.* **116** 411